J. Cell. Mol. Med. Vol 13, No 4, 2009 pp. 664-679

Intracardiac injection of erythropoietin induces stem cell recruitment and improves cardiac functions in a rat myocardial infarction model

Christian Klopsch [a, #], Dario Furlani [a, #], Ralf Gäbel [a], Wenzhong Li [a, *], Erik Pittermann [a], Murat Ugurlucan [a], Guenther Kundt [b], Christiana Zingler [c], Ulf Titze [d], Weiwei Wang [a], Lee-Lee Ong [a], Klaus Wagner [f], Ren-Ke Li [g], Nan Ma [a, e, †, *], Gustav Steinhoff [a, †]

[a] Department of Cardiac Surgery, University of Rostock, Rostock, Germany
[b] Institute of Medical Informatics and Biometry, University of Rostock, Rostock, Germany
[c] Institute of Clinical Chemistry and Laboratory Medicine, University of Rostock, Rostock, Germany
[d] Institute of Pathology, University of Rostock, Rostock, Germany
[e] Zentrum für Biomaterialentwicklung, GKSS, Teltow, Germany
[f] Department of Anesthesia, Klinikum Südstadt, Rostock, Germany
[g] Division of Cardiac Surgery, Toronto General Hospital and the University of Toronto, Toronto, Canada

Received: July 12, 2008; Accepted: September 23, 2008

Abstract

Erythropoietin (EPO) protects the myocardium from ischaemic injury and promotes beneficial remodelling. We assessed the therapeutic efficacy of intracardiac EPO injection and EPO-mediated stem cell homing in a rat myocardial infarction (MI) model. Following MI, EPO (3000 U/kg) or saline was delivered by intracardiac injection. Compared to myocardial infarction control group (MIC), EPO significantly improved left ventricular function ($n = 11–14$, $P < 0.05$) and decreased right ventricular wall stress ($n = 8$, $P < 0.05$) assessed by pressure-volume loops after 6 weeks. MI-EPO hearts exhibited smaller infarction size (20.1 ± 1.1% *versus* 27.8 ± 1.2%; $n = 6–8$, $P < 0.001$) and greater capillary density (338.5 ± 14.7 *versus* 259.8 ± 9.2 vessels per mm^2; $n = 6–8$, $P < 0.001$) than MIC hearts. Direct EPO injection reduced post-MI myocardial apoptosis by approximately 41% (0.27 ± 0.03% *versus* 0.42 ± 0.03%; $n = 6$, $P = 0.005$). The chemoattractant SDF-1 was up-regulated significantly assessed by quantitative real-time PCR and immunohistology. c-Kit$^+$ and CD34$^+$ stem cells were significantly more numerous in MI-EPO than in MIC at 24 hrs in peripheral blood ($n = 7$, $P < 0.05$) and 48 hrs in the infarcted hearts ($n = 6$, $P < 0.001$). Further, the mRNAs of Akt, eNOS and EPO receptor were significantly enhanced in MI-EPO hearts ($n = 7$, $P < 0.05$). Intracardiac EPO injection restores myocardial functions following MI, which may attribute to the improved early recruitment of c-Kit$^+$ and CD34$^+$ stem cells *via* the enhanced expression of chemoattractant SDF-1.

Keywords: cardiac regeneration • ischaemia • chemoattractant • stem and progenitor cells

Introduction

Erythropoietin (EPO) is a hypoxia-induced glycoprotein hormone that stimulates the proliferation and differentiation of erythroid precursor cells in order to counteract diminished oxygen levels, including those caused by anaemia and hypoxia [1, 2]. It can inhibit hypoxia-induced apoptosis of cardiomyocytes and protect cardiomyoblasts from hydrogen peroxide-induced injury [3–5]. EPO can also induce neo-vascularization [6], reduce the infarction size and confer effective cardiac protection against ischaemia-reperfusion injury and chronic heart failure [7–10]. This combined evidence has fuelled significant interest in the potential use of EPO as a cytoprotective agent in the cardiovascular system.

[#,†]Authors contributed equally to this work.
*Correspondence to: Dr. Nan MA and Dr. Wenzhong LI,
Department of Cardiac Surgery, University of Rostock,
Schillingallee 35, 18057 Rostock, Germany.
Tel.: +49 381 494 61 00
Fax: +49 381 494 61 02
E-mail: nan.ma@med.uni-rostock.de; wenzhong.li@med.uni-rostock.de

doi:10.1111/j.1582-4934.2008.00546.x

Numerous studies reveal that transplantation of endothelial progenitor cells (EPCs) isolated from bone marrow (BM) and peripheral blood results in neovascularization of the ischaemic tissues [11–17]. Current findings demonstrate EPO treatment can mobilize EPCs in animals and humans [18–20] and increase the adhesive and proliferative properties of circulating EPCs [21]. However, it is still not clear whether EPO-mobilized EPCs can migrate into the ischaemic myocardium and participate in the process of myocardial regeneration.

Therefore, we evaluated the therapeutic efficacy of intracardiac EPO injection in the infarcted heart. We assessed if intracardiac injection of EPO could recruit stem and progenitor cells to the infarcted heart by activating stem cell homing signalling to promote cardiac regeneration after myocardial infarction (MI).

Materials and methods

Experimental design

Surgical and animal care protocols were reviewed and approved by the local animal care committees of Mecklenburg/Vorpommern. Lewis rats (male, 289.5 ± 9.0 g, Charles River Laboratories, Sulzfeld, Germany) were randomly assigned to three groups: Sham operation (Sham, $n = 55$), MI followed with EPO treatment (MI-EPO, $n = 99$) and saline injected MI control group (MIC, $n = 95$). A subset of randomly selected rats from the MIC and MI-EPO groups were sacrificed for haematological, biochemical and fluorescence-activated cell sorting (FACS) analysis at 24 hrs, 48 hrs and 2 weeks after coronary artery ligation. For histological and real-time polymerase chain reaction (real-time PCR) evaluation, rats were killed at 24 hrs and 48 hrs, respectively. The remaining rats were assessed at 6 weeks for functional measurement, heart weight and histological analysis.

Generation of MI in rats and EPO injection

Rats were anaesthetized with sodium pentobarbital (Sigma-Aldrich, St. Louis, MO, USA; 50 mg/kg, intraperitoneal administration) and the left anterior descending coronary artery (LAD) was permanently ligated 2 mm beyond its origin. Immediately after LAD ligation, rats received 4 intramyocardial injections (25 μl each) of either recombinant human EPO (Epoetin-α/Erypo®, Ortho Biotech, Neuss, Germany) at a total dosage of 3000U/kg dissolved in 0.9% saline, or saline solution alone. Injections were given along the border of the blanched myocardium. Sham-operated rats underwent identical surgical procedures without permanent LAD ligation but followed by intramyocardial saline injections.

Haematological, biochemical and FACS analysis of peripheral blood

Analysis of peripheral blood from the right ventricle (MIC and MI-EPO groups) were performed at 24 hrs ($n = 7$, for each group), 48 hrs ($n = 7$) and 2 weeks ($n = 5$) after MI. Haematocrit was examined by Sysmex XE-2100 (SYSMEX, Norderstedt, Germany). Plasma concentration of EPO was evaluated with Enzyme-linked Immunosorbent Assay (ELISA) kits using Immulite Fa.DPC (Siemens, Bad Nauheim, Germany) and mouse anti-EPO monoclonal antibody (Euro/DPC, Gwynedd, UK). Plasma concentration of cardiac Troponin T (cTnT) was also analysed with ELISA using Elecsys 2010 (F. Hoffmann-La Roche, Basel, Switzerland) and mouse anti-cTnT monoclonal antibody (Roche Diagnostics, Mannheim, Germany). To examine the effects of EPO treatment on stem cell mobilization, nucleated cell fraction of peripheral blood was separated for flow cytometry analysis. Cells were incubated with rabbit anti-c-Kit or goat anti-CD34 polyclonal antibodies (Santa Cruz, Santa Cruz, CA, USA) following lysis of erythrocytes with FACS-Lysing solution (Becton Dickinson, Mountain View, CA, USA). Subsequently, donkey anti-rabbit Alexa-Fluor 488 or donkey anti-goat Alexa-Fluor 568 conjugated secondary antibodies (Invitrogen, Carlsbad, CA, USA) were applied to the samples. The number of c-Kit$^+$ and CD34$^+$ cells in the nucleated cell fraction of peripheral blood was examined by FACS (Calibur; Becton Dickinson).

Quantitative real-time PCR analysis

For analysis of mRNA levels, hearts of 24 hrs ($n = 7$, for each group), 48 hrs ($n = 7$) and 6 weeks ($n = 6$) post-infarction were removed and the left ventricle (LV) was carefully dissected along the right ventricular free wall. The infarcted zone (IZ) from the external wall of LV and the non-infarcted zone (NIZ) from the remote myocardium of the interventricular septum were separated and snap-frozen in liquid nitrogen. Total RNA was isolated following the instructions of the TRIZOL® Reagent (Invitrogen) including DNase treatment. Primer sets for real-time PCR (Applied Biosystems Foster City, CA, USA) are summarized in Table S1. Amplification and detection were performed with the StepOnePlus™ Real-Time PCR System (Applied Biosystems) in TaqMan Universal Master Mix (Applied Biosystems) according to the instructions of the manufacturer (Applied Biosystems) and repeated at least three times using the following program: 1 cycle of 50°C for 2 min., 1 cycle of 95°C for 10 min. and 40 cycles of 95°C for 15 sec. and 60°C for 1 min. DNA extracts were tested in at least triplicate and negative controls were included in each assay. Cycle thresholds (C_T) for single reactions were determined with StepOne™ Software 2.0 (Applied Biosystems) and the target genes were normalized against GAPDH (formula: $\Delta C_T = C_{T\,target} - C_{T\,GAPDH}$). Resulting ΔC_T of triplicates was averaged and $\Delta\Delta C_T$ were obtained using Sham group as calibrator sample (formula: $\Delta\Delta C_T = \Delta C_{T\,sample} - \Delta C_{T\,calibrator\,sample}$). In the current study, the $2^{-\Delta\Delta C}$ method [22] was employed to present the changes in gene expression after MI and EPO treatment.

Immunohistochemistry

For immunohistological detection of c-Kit$^+$ and CD34$^+$ stem cells, frozen transverse tissue sections (5 μm) of hearts from MIC and MI-EPO ($n = 6$ for each time point and group) were incubated with rabbit anti-c-Kit or goat anti-CD34 polyclonal antibodies. Reactivity of employed anti-CD34 antibody with endothelial cells was tested by double-staining with goat anti-CD31 polyclonal antibody (Santa Cruz). Subsequently, the sections were incubated with donkey anti-rabbit Alexa-Fluor 488 conjugated and donkey anti-goat Alexa-Fluor 488 conjugated secondary antibodies (Invitrogen). Nuclei were counterstained with TOPRO3 (Invitrogen). Labelled sections were observed using a Leica SP2 Confocal Microscope (Leica, Hamburg, Germany). The number of c-Kit$^+$ and CD34$^+$ cells were counted in 20 randomly chosen high-power fields (HPFs, 630×) of NIZ and IZ. Results were

expressed as cells per HPF. Moreover, we performed double immunostaining between stromal cell-derived factor 1 (SDF-1) (Primary antibody: monoclonal mouse anti-SDF-1, clone 79018, R&D Systems, Minneapolis, MN, USA; Secondary antibody: Alexa-Fluor 647 conjugated goat anti-mouse IgG, Invitrogen) and endothelial cell marker CD31 (Primary antibody: polyclonal goat anti-CD31; Secondary antibody: Alexa-Fluor 488 donkey anti-goat IgG). Nuclei were counterstained with 6-diamidino-2-phenylindole (DAPI; Sigma-Aldrich). All morphometric studies were performed by two examiners who were blinded to the treatment.

Left and right ventricular catheterization

Six weeks after surgery, rats (Sham $n = 11$, MIC $n = 14$, MI-EPO $n = 11$) underwent pressure-volume loop (P/V loop) measurements according to the protocol of CardioDynamics BV (CD Leycom, Zoetermeer, The Netherlands). Data were collected with the Millar Pressure-Volume System (Ultra-Miniature Pressure-Volume Catheter (model SPR-838), Millar Pressure Conductance Unit (model MPCU-200) and Millar PowerLab data-acquisition hardware; emka Technologies, Paris, France). Calibration of pressure and volume was performed by equating the minimal and maximal conductances with minimal (0 mmHg) and maximal (100 mmHg) pressures as well as minimal and maximal blood volumes received from venous circulation. After inserting the catheter into carotid artery retrograde access to the LV was achieved. Volume signal was corrected by measurement of wall conductance (parallel volume; Vp) *via* hypertonic saline (5%) injection. P/V loops of the LV were recorded under normal conditions (baseline) followed by stress conditions mediated by intravenous dobutamine administration (10 μg/kg/min., Sigma-Aldrich). Then the animal was allowed to rest for 30 min. until the systemic hemodynamic condition was stable at baseline level, which was confirmed by permanent monitoring *via* conductance catheterization. Thereafter, the catheter was removed and open-chest right ventricular catheterization was carried out as described elsewhere [23]. Right ventricular P/V loop analyses (Sham $n = 5$, MIC $n = 8$, MI-EPO $n = 8$) were performed under baseline conditions. Data were analysed with IOX Version 1.8.3.20 software (emka Technologies).

Infarction size, cardiac remodelling and cardiomyocyte apoptosis analyses

After P/V loop measurements, rats were sacrificed. Each heart was removed and ventricles were dissected as described in real-time PCR method part. The body weight (BW), heart weight (HW), right ventricular free wall weight and LV weight were determined to the nearest milligram (Sham $n = 11$, MIC $n = 14$, MI-EPO $n = 11$). The LV (Sham $n = 6$, MIC $n = 8$, MI-EPO $n = 6$) was embedded in paraffin and sliced horizontally for histological analysis. Formalin-fixed LV transverse tissue sections (5 μm thick) of 8 levels (15 mm thick) were stained with Fast Green FCF (Sigma-Aldrich) and Sirius Red (Division Chroma, Muenster, Germany). Sirius Red positive areas (infarction size) were analysed using the computerized planimetry (Axio Vision LE Rel. 4.5 software; Zeiss, Jena, Germany). To determine the LV wall thickness in the remote area (RA), 4 independent measurements were performed on each level of every heart and averaged. The LV wall thickness in IZ was determined similarly by three measurements.

To evaluate collagen density and cardiomyocyte size of viable myocardium ($n = 6$, for each group), LV transverse tissue sections stained with Fast Green FCF and Sirius Red were analysed using computerized planimetry [24]. Sirius Red positive areas in the RA near endocardial border were examined in 10 randomly chosen fields per section (one section per level) at 200× magnification. Collagen density was expressed as the ratio of collagen area to myocardial area in percentage. The size of Fast Green FCF positive cardiomyocytes in RA near endocardial border was studied in parallel, employing 400× magnification as previously described [24]. One hundred cardiomyocytes were randomly chosen and measured by computerized planimetry.

To analyse the cardiomyocyte apoptosis, transverse sections from the mid portions of LV (level four and five) underwent TUNEL (terminal deoxynucleotidyl transferase-mediated dUTP nick end-labelling assay) assay according to the manufacturer's instructions (*In situ* cell death detection kit, Fluorescein, Roche Diagnostics). Subsequently, slides were stained with mouse monoclonal anti-cardiac myosin primary antibody (Millipore, Billerica, USA) and goat anti-mouse Alexa-Fluor 568 conjugated secondary antibody (Invitrogen), counterstained with TOPRO3 for nuclei and examined with confocal microscope. The number of TUNEL-positive cardiomyocytes was counted in 16 randomly chosen HPFs (630×) per section (one section per level) for both RA and border zone ($n = 6$, for each group). Results were expressed as the proportion of the TUNEL-positive cardiomyocyte nuclei to the total number of cardiomyocytes in percentage. All parameters were analysed by a researcher blinded to the treatment.

Determination of capillary density

Capillary density was assessed at 6 weeks after surgery by counting the number of capillaries of the heart sections immunostained with polyclonal goat anti-CD31 primary antibody followed by donkey anti-goat Alexa-Fluor 568 conjugated secondary antibody. Sections were counterstained with DAPI. Five sections within the border zone and RA of each animal (Sham $n = 6$, MIC $n = 8$, MI-EPO $n = 6$) were analysed. Capillaries were counted in 16 (RA) or 8 (border zone) randomly chosen fields (400×). Results were expressed as capillaries per mm^2.

Statistical analyses

Statistical analyses were performed using Sigma Stat software version 3.0 (SPSS Inc., Chicago, IL, USA). Results are expressed as mean ± S.E.M. Overall comparisons of the treatment groups were performed by using the one-way analyses of variance (ANOVA) method that applies *post hoc* multiple Holm–Sidak tests, and by using the nonparametric Kruskal–Wallis (failing normality) or *post hoc* multiple Dunn tests. *P*-values <0.05 were considered statistically significant.

Results

Local EPO delivery improves cardiac functions

Erythropoietin-α treatment enhanced systolic and diastolic properties of the infarcted LV both at baseline and under stress conditions. Hemodynamic changes are summarized in Table 1 (baseline) and Table 2 (dobutamine stress). EPO treatment produced a 53% increase in LV ejection fraction (LV-EF, $P = 0.003$, Fig. 1A), a 2-fold increase in LV stroke work and a 61% increase in

Table 1 Hemodynamics of the LV under baseline conditions 6 weeks after MI

Parameter	Sham ($n = 11$)	MIC ($n = 14$)	MI-EPO ($n = 11$)	P*
Pmax (mmHg)	147.74 ± 3.36	114.95 ± 6.94	126.70 ± 7.12	0.255
dp/dt max (mmHg/sec.)	10942.50 ± 276.37	5815.23 ± 335.97	7374.84 ± 525.45	0.016
-dp/dt max (mmHg/sec.)	−10137.44 ± 281.57	–3453.68 ± 121.38	–4743.93 ± 480.98	0.007
Relaxation time (msec)	8.05 ± 1.53	19.74 ± 1.40	13.07 ± 1.37	0.003
EDV (μl)	211.30 ± 14.62	312.44 ± 27.98	313.56 ± 23.52	0.784
ESV (μl)	103.24 ± 5.96	225.36 ± 20.04	187.49 ± 15.60	0.101
SV (μl)	108.06 ± 10.31	87.11 ± 11.52	126.07 ± 12.18	0.031
EF (%)	50.45 ± 2.08	27.12 ± 1.78	40.05 ± 2.42	<0.001
SW (μlxmmHg)	13124.94 ± 1694.95	6166.67 ± 846.91	11742.17 ± 1352.87	0.001
HR (1/min.)	418.16 ± 10.19	359.61 ± 19.73	409.09 ± 11.32	0.055

Values are represented as mean ± S.E.M., * MIC *versus* MI-EPO, Pmax means maximum pressure; dp/dt indicates peak rate of maximum pressure rise (dp/dt max) and decline (−dp/dt max); EDV, end-diastolic volume; ESV, end-systolic volume; SV, stroke volume; EF, ejection fraction; SW, stroke work; and HR, heart rate.

Table 2 Hemodynamics of the LV under stress conditions 6 weeks after MI

Parameter	Sham ($n = 11$)	MIC ($n = 14$)	MI-EPO ($n = 11$)	P*
Pmax (mmHg)	144.54 ± 3.74	124.08 ± 3.34	131.05 ± 4.37	0.209
dp/dt max (mmHg/sec.)	18962.22 ± 358.66	9529.60 ± 490.22	12456.81 ± 726.55	0.002
-dp/dt max (mmHg/sec.)	−9418.62 ± 349.47	−5421.46 ± 355.71	−6741.31 ± 538.93	0.045
Relaxation time (msec)	5.95 ± 1.04	13.76 ± 1.51	8.92 ± 1.13	0.022
EDV (μl)	186.24 ± 14.14	299.74 ± 30.16	315.01 ± 16.06	0.684
ESV (μl)	48.08 ± 5.23	203.67 ± 21.44	160.20 ± 16.02	0.136
SV (μl)	138.06 ± 10.06	96.13 ± 13.37	154.77 ± 20.15	0.019
EF (%)	74.44 ± 1.54	31.61 ± 2.25	48.39 ± 5.01	0.003
SW (μlxmmHg)	16336.62 ± 1334.16	7428.62 ± 1050.69	14937.78 ± 1971.47	0.004
HR (1/min.)	474.30 ± 10.06	429.92 ± 8.29	459.30 ± 7.85	0.019

Values are represented as mean ± S.E.M., * MIC *versus* MI-EPO, Pmax means maximum pressure; dp/dt indicates peak rate of maximum pressure rise (dp/dt max) and decline (-dp/dt max); EDV, end-diastolic volume; ESV, end-systolic volume; SV, stroke volume; EF, ejection fraction; SW, stroke work; and HR, heart rate.

LV stroke volume relative to MIC ($P = 0.004$, $P = 0.019$, Table 2) under stress conditions. Left ventricular peak rate of pressure rise (LV dp/dt max, Fig. 1A), a commonly used index of myocardial contractility, was significantly enhanced at baseline ($P = 0.016$) and under stress ($P = 0.002$) when compared with MIC. Moreover, we also observed a 24% increase in the peak rate of LV pressure decline (LV -dp/dt max) compared with MIC (Fig. 1A) under stress conditions, demonstrating enhanced relaxation in MI-EPO. Speed of relaxation in MIC was significantly lower both at baseline ($P = 0.007$) and under dobutamine stress ($P = 0.045$, Tables 1 and 2). Accordingly, LV relaxation time was longer (baseline: $P = 0.003$; stress: $P = 0.022$) in MIC than in MI-EPO hearts. Thus, EPO significantly improved contractility, reduced stiffness and improved elasticity of the LV. Representative single left ventricular heart beats are visualized in Fig. 1B. With respect to the performance of the right ventricle (RV), EPO improved significantly right ventricular loading conditions. RV maximum pressure (RV-Pmax) and RV end-systolic pressure (RV-ESP), whose elevations are consistent with pulmonary hypertension, were both reduced under baseline conditions in MI-EPO compared with MIC ($P = 0.005$, $P = 0.003$, Fig. 1A and B). However, RV dp/dt max did not significantly differ between the two groups ($P = 0.199$). MI-EPO hearts responded to dobutamine stress with a significant increase in heart rate ($P = 0.019$, Table 2). Taken together, these results demonstrate that direct administration of EPO improved both left and right ventricular performance.

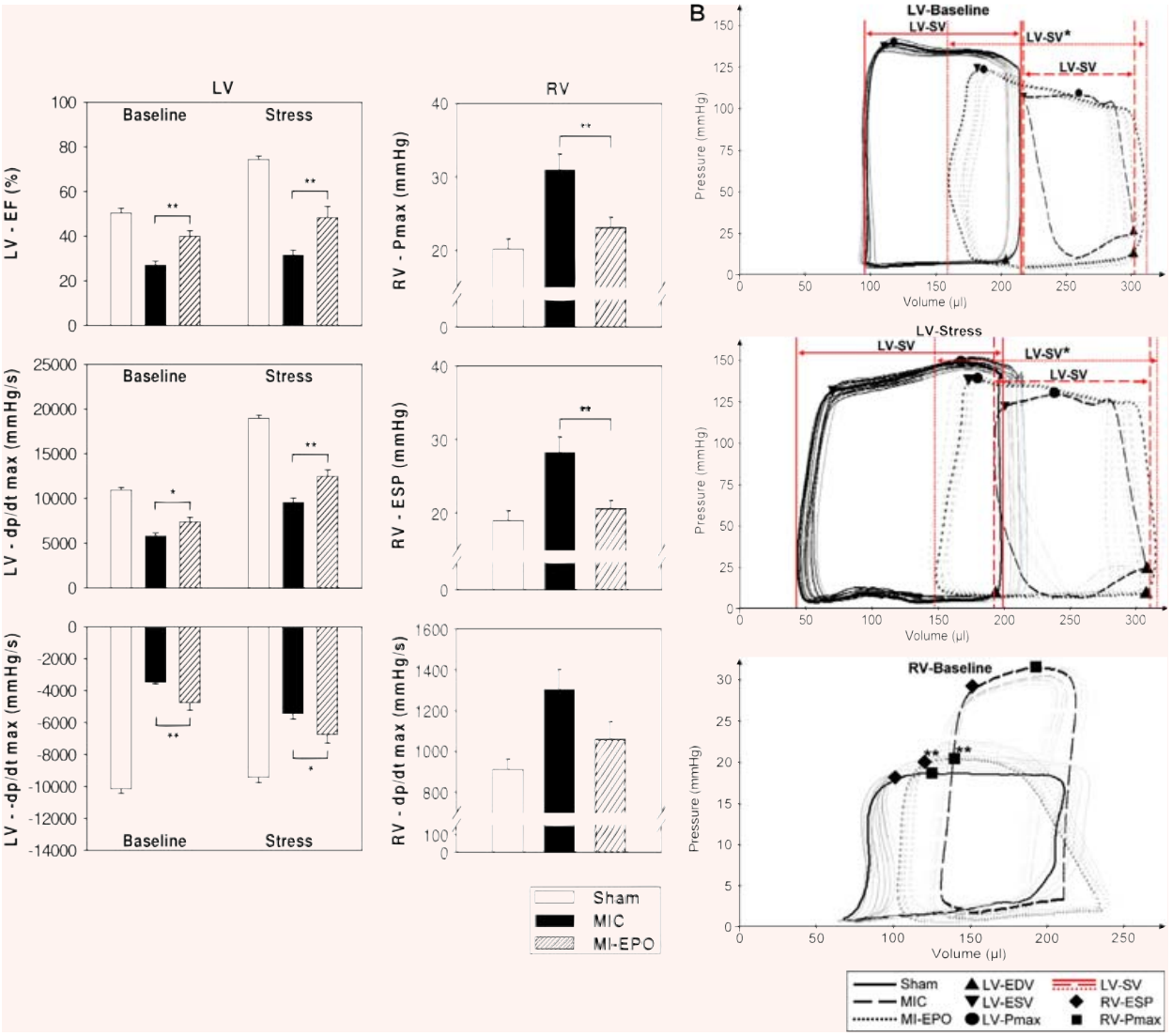

Fig. 1 Direct EPO injection restored cardiac functions 6 weeks after MI assessed by catheterization. (**A**) Left ventricular function (Sham $n = 11$, MIC $n = 14$, MI-EPO $n = 11$) at both baseline and stress conditions (left panel) as well as right ventricular function (Sham $n = 5$, MIC $n = 8$, MI-EPO $n = 8$) at baseline condition (right panel). (**B**) Representative single heart beat obtained from Sham (solid loops), MIC (dashed loops) and MI-EPO (dotted loops) hearts revealed the increments of left ventricular stroke volume (LV-SV) in MI-EPO compared with MIC under baseline (upper panel) and dobutamine stress (middle panel) conditions. RV examinations (lower panel) displayed the reductions of right ventricular maximum pressure (RV-Pmax) and end-systolic pressure (RV-ESP) in MI-EPO compared with MIC under baseline conditions. $*P < 0.05$ MIC *versus* MI-EPO, $**P < 0.01$ MIC *versus* MI-EPO.

Local EPO delivery reduces infarction size, inhibits cardiac remodelling and cardiomyocytes apoptosis

Computerized planimetry of the heart cross-sections revealed that scar area was remarkably lower in MI-EPO than in MIC (Fig. 2A and B). The average infarction size decreased significantly from 27.76 ± 1.20% in MIC to 20.11 ± 1.13% in MI-EPO ($P < 0.001$, Fig. 2C). Moreover, the interventricular septum thickness of EPO-treated rats in the RA was decreased compared with MIC rats ($P = 0.014$, Fig. 2D). Wall thickness in the infarcted area did not differ among experimental groups ($P = 0.109$). Furthermore, EPO-treated rats showed a 12% reduction in heart weight-to-body weight (HW/BW) ratio ($P = 0.003$, Fig. 2E), a commonly used index of cardiac hypertrophy. Therefore, these results suggest that EPO limits the development of post-infarction hypertrophy. More specifically, we found a 26% reduction in right ventricular free wall weight-to-body weight (RVW/BW) ratio ($P = 0.041$, Fig. 2F) in

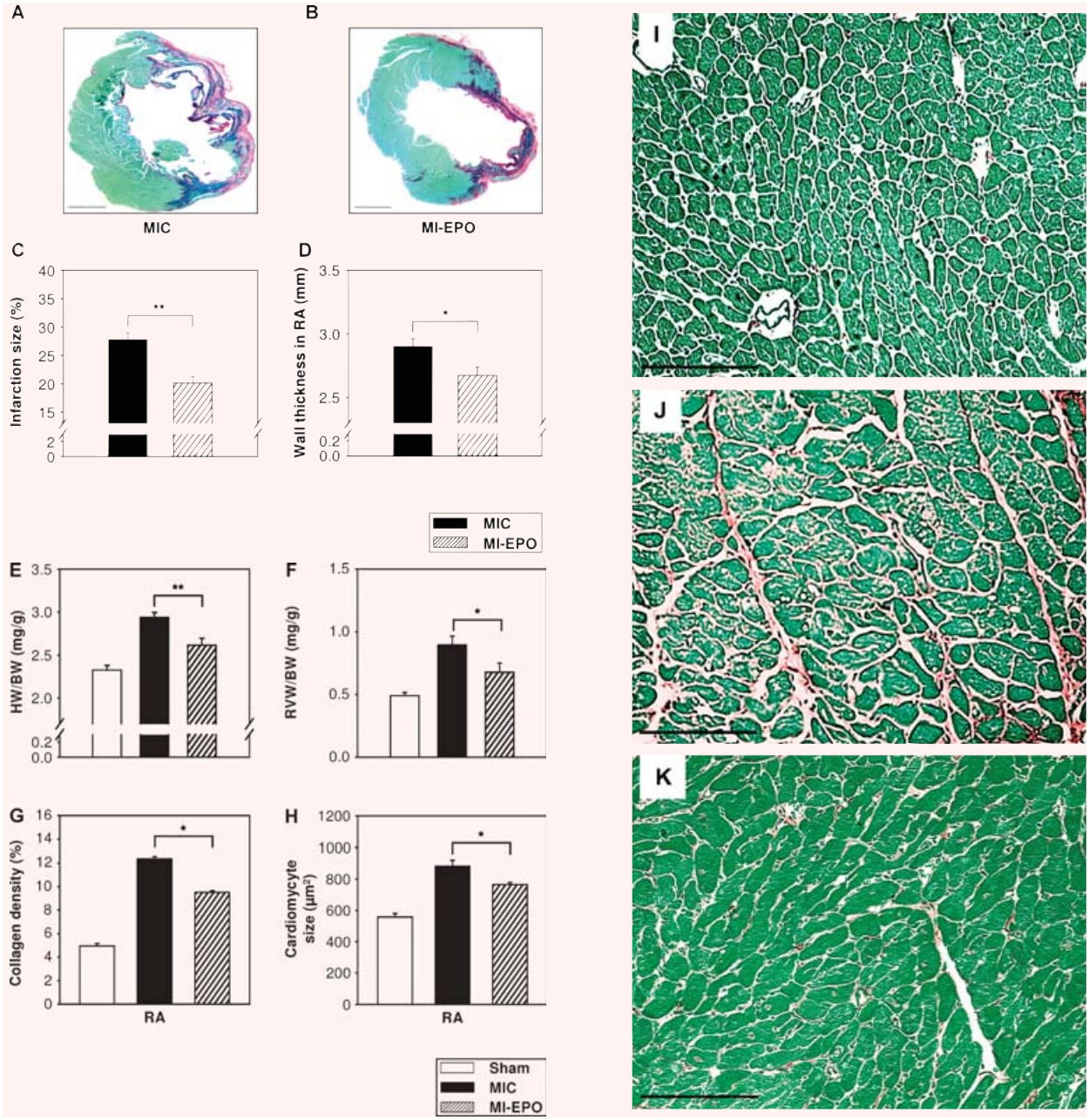

Fig. 2 Effects of direct EPO injection on cardiac remodelling 6 weeks after MI. (**A, B**) Representative left ventricular cross-sections stained with Sirius Red (red, fibrosis) and Fast Green FCF (green, myocytes) from rats without (left) and with (right) EPO treatment. (**C**) Ratio of infarction area to entire LV is decreased in MI-EPO ($n = 6$) compared with MIC ($n = 8$). (**D**) Wall thickness of RA is significantly reduced in MI-EPO ($n = 6$) compared with MIC ($n = 8$). (**E, F**) EPO treatment results in a significantly decreased HW/BW ratio, and RVW/BW ratio (Sham $n = 11$, MIC $n = 14$, MI-EPO $n = 11$). (**G, H**) Collagen density (**G**) and cardiomyocyte size (**H**) in RA of MI-EPO hearts ($n = 6$) were reduced compared with MIC ($n = 6$). (**I–K**) Representative staining for Sirius Red (red, fibrosis) and Fast Green FCF (green, myocytes) in the RA of Sham (I, upper panel), MIC (J, middle panel) and MI-EPO (K, lower panel). Scale bars = 150 μm. (**L, M**) Representative immunostaining for TUNEL (green, square) and cardiac myosin (red) in RA (L, upper panel) and the border zone (M, lower panel) of MIC hearts. Scale bars = 25 μm (left panel). Scale bars = 5 μm (right panel). Blue, TOPRO3 in nuclei. (**N**) Cardiomyocyte apoptosis was reduced in both the border zone (left) and the RA (right) in MI-EPO ($n = 6$) compared with MIC ($n = 6$). (**O**) Quantitative real-time PCR analysis for Bcl2 gene in the IZ (left) and NIZ (right) of MI-EPO ($n = 6$), MIC ($n = 6$) and Sham ($n = 6$) hearts. The average mRNA expression level in the sham hearts was arbitrarily given a value of 1 (2°). $^{*}P < 0.05$, $^{**}P < 0.01$.

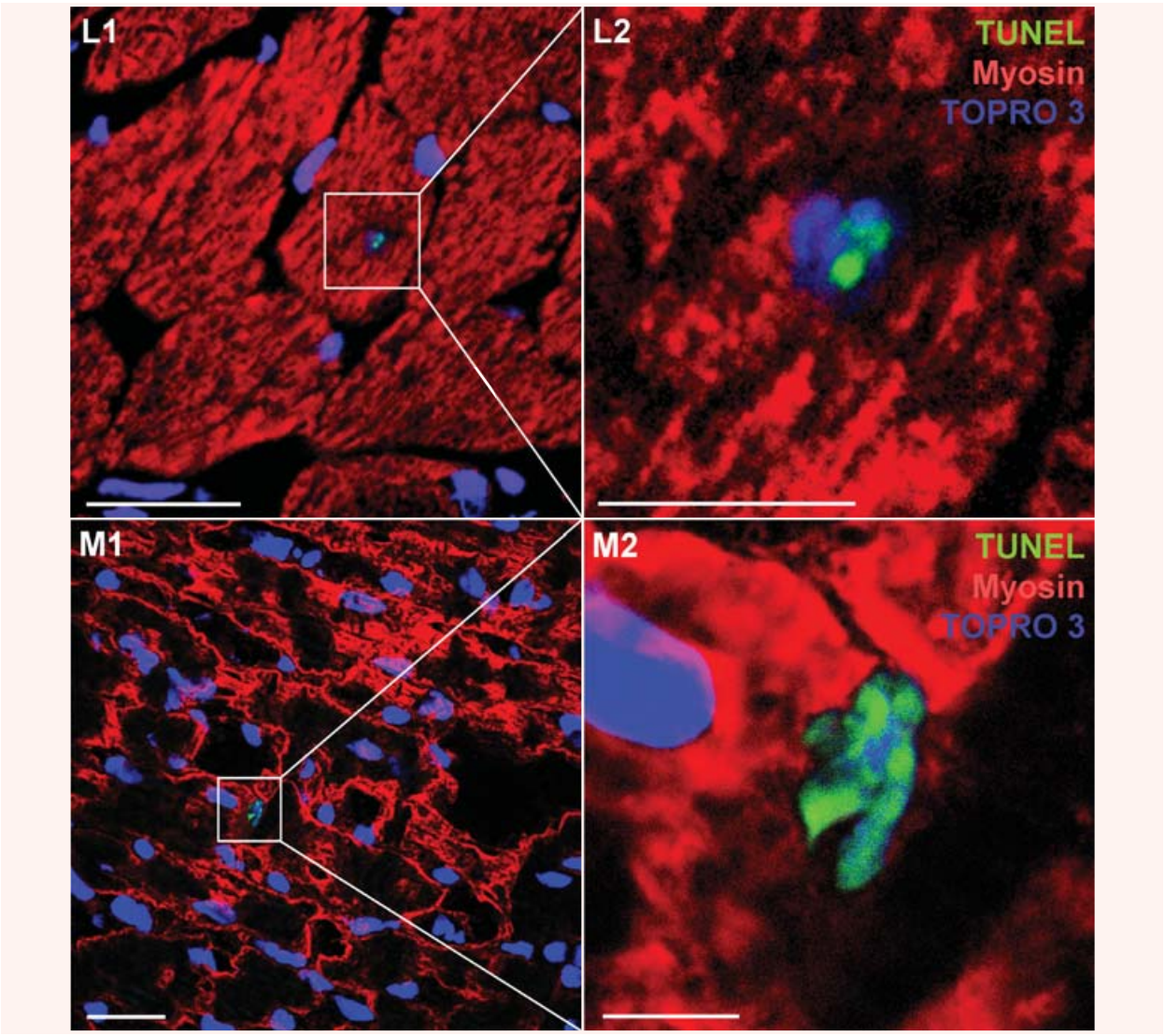

Fig. 2 Continued

MI-EPO, another highly reliable indicator of reduced left ventricular decompensation. There was no significant reduction in left ventricular weight-to-body weight (LVW/BW) ratio in EPO-treated rats ($P = 0.061$). Body weight did not differ among experimental groups. Collagen density in RA decreased significantly from 12.36 ± 0.20% in MIC to 9.53 ± 0.13% in MI-EPO ($P < 0.001$, Fig. 2G, I–K). Average cardiomyocyte size was significantly smaller in MI-EPO (765.21 ± 13.74μm^2) when compared to MIC (882.98 ± 36.91μm^2) ($P = 0.015$, Fig. 2H, I–K). Further, percentage of apoptotic cardiomyocyte reduced from 0.19 ± 0.02% (MIC group) to 0.12 ± 0.01% (MI-EPO group, $P = 0.023$) in RA and from 0.42 ± 0.03% (MIC group) to 0.27 ± 0.03% (MI-EPO group, $P = 0.005$) in the border zone (Fig. 2L–N). Quantitative real-time PCR revealed a 3-fold increase in mRNA expression of pro-survival Bcl2 gene after 6 weeks in the non-infarcted myocardium of MI-EPO hearts compared with MIC hearts ($P = 0.001$, Fig. 2O).

Local EPO delivery promotes neoangiogenesis

Capillary density was analysed by immunostaining with an anti-CD31 antibody (Fig. 3A). Capillary density was significantly higher in both zones for rats that received EPO (border zone: $P < 0.001$; RA: $P = 0.009$, Fig. 3B). There was no sign of intramural thrombosis after EPO injection.

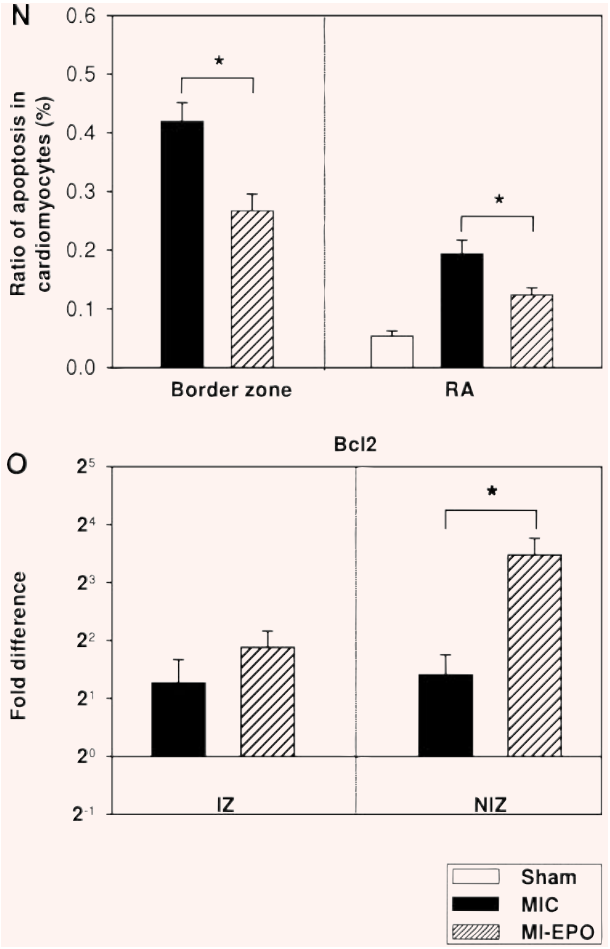

Fig. 2 Continued

Local EPO delivery up-regulates SDF-1, CXCR4 and MMP-2 expression

We examined whether EPO treatment altered SDF-1, CXCR4 and MMP2 expression by immunostaining and real-time PCR. Quantitative real-time PCR revealed SDF-1 mRNA was significantly up-regulated in MI-EPO hearts ($P < 0.05$, Fig. 4A) at 24 hrs in both IZ and NIZ compared with MIC. These data were further corroborated by immunostaining of SDF-1, which identified a clear SDF-1 expression pattern in MI-EPO hearts: in NIZ, SDF-1 was detected in the endothelial cells bordering the vessel lumen (Fig. 4D–G). In IZ, SDF-1 was detected in interstitial cells and endothelial cells (Fig. 4H and I). More abundant SDF-1 signals were detected in IZ of MI-EPO hearts compared with MIC (Fig. 4J and K). Furthermore, the mRNA of CXCR-4 and matrix metalloproteinase 2 (MMP-2) augmented at 24 hrs in NIZ. In IZ, the CXCR4 and MMP-2 mRNA levels did not differ between MIC and MI-EPO (Fig. 4B and C).

Local EPO delivery augments sequential myocardial stem cell recruitment

Given the potential role of the stem cell recruitment by EPO, c-Kit$^+$ and CD34$^+$ cell number and mRNA level in the heart were assessed by immunostaining and quantitative real-time PCR. At 24 hrs c-Kit mRNA in MI-EPO hearts was significantly up-regulated in IZ. In both IZ and NIZ, c-Kit mRNA in MI-EPO hearts was markedly higher compared with MIC at 48 hrs ($P < 0.05$, Fig. 5A). There was an 80% increase of c-Kit$^+$ cells after injection at 48 hrs in IZ ($P < 0.001$, Fig. 5E) detected by immunostaining. Similarly, CD34 mRNA in both IZ and NIZ of MI-EPO rats was up-regulated compared with MIC at 24 hrs ($P < 0.05$, Fig. 5B). Immunostaining, which was devoid of CD31 reactivity, revealed 72% increase of CD34$^+$ cells in MI-EPO at 48 hrs in IZ ($P = 0.001$; Fig. 5H). These observations therefore revealed that EPO may enhance stem cell recruitment on the acute phase post-MI.

Local EPO delivery induces survival pathways

To clarify cardioprotective effects of EPO, quantitative real-time PCR was applied to evaluate mRNA levels of eNOS and Akt, known to be involved in various steps of anti-inflammation, anti-apoptosis and myocyte survival. As shown in Fig. 6A and B, mRNA levels of Akt and eNOS were up-regulated in both IZ and NIZ at 24 and 48 hrs in response to EPO treatment ($P < 0.05$). Thus, the cardioprotective effects of direct EPO injection may be associated with the up-regulation of tissue protective factors like Akt and eNOS.

Local EPO delivery up-regulates EPO receptor

We performed real-time PCR to estimate the effect of direct EPO injections on EPO-R in cardiac tissue. EPO-R mRNA of MI-EPO was significantly up-regulated in IZ at 24 hrs, and in NIZ at both 24 and 48 hrs as compared with MIC ($P < 0.05$, Fig. 6C).

Local EPO delivery mobilizes stem/progenitor cells to peripheral blood

Local delivery of EPO enhanced c-Kit$^+$ and CD34$^+$ cell mobilization to the peripheral blood at 24 hrs. The mean percentages of c-Kit$^+$ and CD34$^+$ cells in the nucleated cell fraction of peripheral blood were increased from 1.74 $\pm$ 0.25% in MIC to 4.78 $\pm$ 1.23% in MI-EPO for c-Kit$^+$ cells ($P = 0.035$) and from 0.56 $\pm$ 0.18% to 1.35 $\pm$ 0.27% for CD34$^+$ cells ($P = 0.029$, Fig. 7A–D).

Local EPO delivery transiently affects haematocrit and reduces cardiac Troponin T

Mean EPO plasma levels in MI-EPO were 282.39 $\pm$ 25.11 mU/ml after 24 hrs and 35.93 $\pm$ 13.04 mU/ml after 48 hrs, and declined

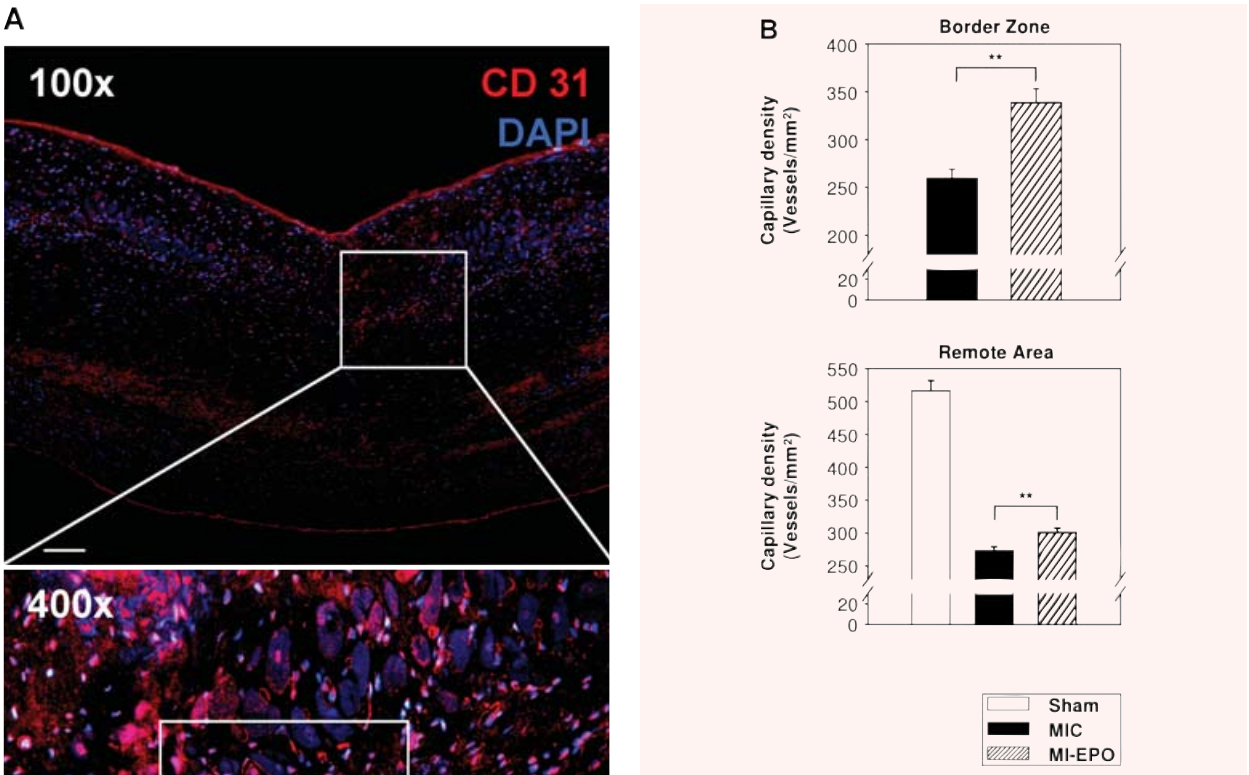

Fig. 3 Direct EPO injection induces neovascularization 6 weeks after MI. (**A**) Endothelial CD31 staining in the infarction area of the LV wall revealed a complex vascular architecture that consisted of regularly shaped vessels (arrows) in MI-EPO, which were not present in MIC. Blue, DAPI in nuclei; 100×, Bar = 100 μm; 400×, Bar = 50 μm; 1000×, Bar = 25 μm. (**B**) Capillary density was significantly higher in MI-EPO ($n = 6$) compared with MIC ($n = 8$) in both the RA and the border zone of the LV. $^{*}P < 0.05$, $^{**}P < 0.01$.

to normal after 2 weeks (Fig. 7E). Haematocrit was transiently elevated by 9.4% (MIC: 0.45 ± 0.01; MI-EPO: 0.50 ± 0.01; $P = 0.004$) at 48 hrs after injection and declined to the level of MIC after 2 weeks (Fig. 7F). Interestingly, plasma levels of cTnT, indicator for myocardial damage related to long-term risk of death from cardiac causes [25], was 3-fold higher in untreated MIC compared to MI-EPO after 2 weeks (MIC: 10.06 ± 0.96 ng/ml; MI-EPO: 3.48 ± 1.49 ng/ml; $P = 0.006$).

Discussion

The current study presents the first time that a single intracardiac administration of EPO after MI significantly up-regulated stem cell homing factor SDF-1 and increased the local numbers of c-Kit^{+} and CD34^{+} stem cells. Local administration of EPO reduced infarction size, inhibited cardiac remodelling, enhanced cardiomyocyte protection and improved cardiac function. Meanwhile, we found

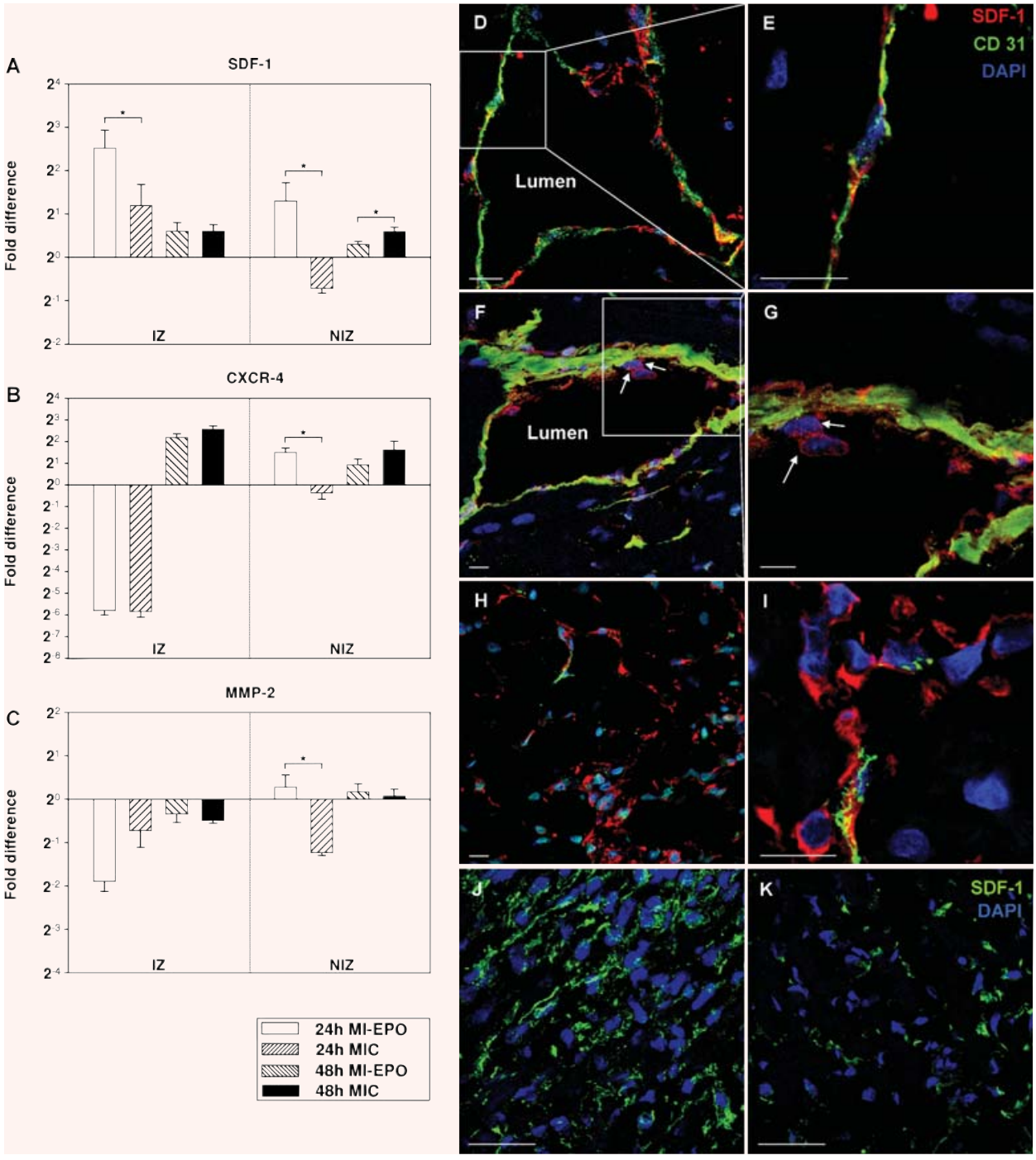

Fig. 4 Direct EPO injection up-regulates SDF-1, CXCR4 and MMP2. (**A–C**) Quantitative real-time PCR analysis for SDF-1 (**A**), CXCR4 (**B**) and MMP2 (**C**) genes, respectively, in IZ and NIZ of MI-EPO ($n = 7$), MIC ($n = 7$) and Sham ($n = 7$) hearts. The average mRNA expression level in the sham hearts was arbitrarily given a value of 1 (2°). *$P < 0.05$. (**D–I**) Representative confocal microscopic images illustrating different expression patterns of SDF-1 in MI-EPO. (**D–G**) In NIZ of MI-EPO, most SDF-1$^+$ cells (red) co-localized with CD31 (green). Occasionally, cell adhesion (arrows in F and G) with the SDF-1$^+$ endothelial cells was visible. (**H, I**) In contrast, a number of SDF-1$^+$ cells (red) in IZ of MI-EPO hearts did not co-localize with CD31 (green). Scale bars = 10 μm. Blue, DAPI in nuclei. (**J, K**) Confocal microscopic images reveal more abundant SDF-1$^+$ signals (green) in IZ of MI-EPO ($n = 6$) than MIC ($n = 6$) hearts after EPO injection. Scale bars = 30 μm. Blue, DAPI in nuclei.

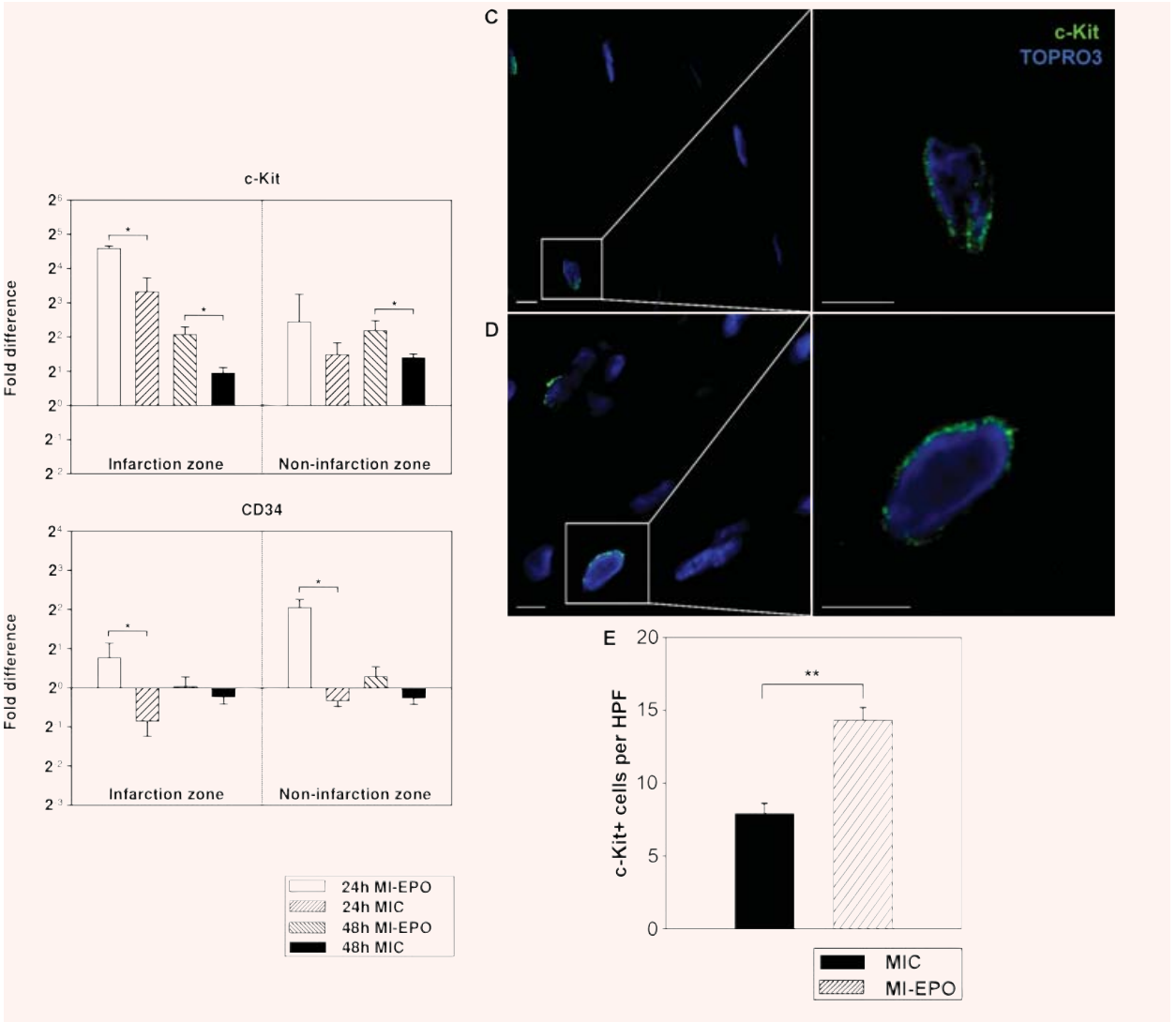

Fig. 5 Direct EPO injection increases c-Kit$^+$ and CD34$^+$ signals. (**A, B**) Quantitative real-time PCR analysis for c-Kit (**A**) and CD34 (**B**) genes in IZ and NIZ of MI-EPO ($n = 7$), MIC ($n = 7$) and Sham ($n = 7$) hearts. The average mRNA expression level of c-Kit and CD34 in the sham hearts was arbitrarily given a value of 1 (2°). *$P < 0.05$. (**C, D**) Representative immunostaining for c-Kit in an EPO-treated heart. c-Kit$^+$ cells (square) were identified in NIZ (**C**) and IZ (**D**) at 48 hrs after treatment. Bar = 5 μm. Blue, TOPRO3 in nuclei. (**E**) The number of c-Kit$^+$ cells per high power field (HPF) in IZ of MI-EPO ($n = 6$) hearts was significantly higher than in MIC ($n = 6$) hearts. **$P < 0.01$. (**F, G**) Representative images for CD34$^+$ (green) cells (square) in NIZ (**F**, Bar = 5 μm) and IZ (**G**, Bar = 10 μm) at 48 hrs after EPO treatment. Red, TOPRO3 in nuclei. (**H**) The number of CD34$^+$ cells per HPF in IZ of MI-EPO ($n = 6$) was significantly higher than in MIC ($n = 6$) hearts. **$P < 0.01$.

reduced cTnT plasma levels and improved RV loading conditions in EPO-treated animals, which may indicate better quality of life and reduced long-term mortality secondary to heart failure [25, 26].

We demonstrate that local EPO delivery improved both left and right ventricular performance. Further, EPO administration inhibited myocardium loss, cardiomyocyte compensatory growth and interstitial fibrosis that was consistent with other studies [3, 27]. Of importance, apoptotic cardiomyocyte in the viable myocardium was significantly reduced even at the late stage of post-MI healing. The significant up-regulation of pro-survival factor Bcl2 mRNA 6 weeks after EPO administration may relate to the long-term anti-apoptotic effects of EPO and the enhanced post-MI cardiomyocyte survival. Eventual consequence of cardiomyocyte loss and LV failure after MI constitutes pulmonary structural remodelling, which contributes to the development of pulmonary hypertension and right ventricular hypertrophy [28]. Elevated RV loading

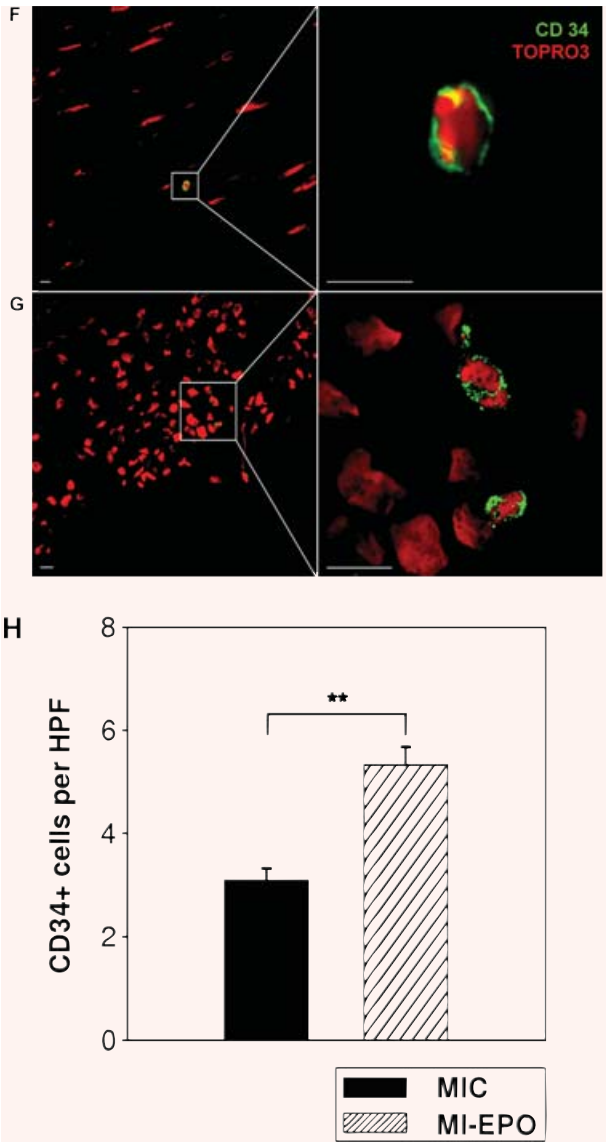

Fig. 5 Continued

conditions are consistent with dyspnoea and related to post-infarction mortality due to global heart failure. We found local EPO injection improved RV loading and delayed RV hypertrophy and therefore may retard heart failure development.

The local administration of EPO described in this report may achieve the same high local concentration possible with a prolonged systemic approach and reduce the complications associated with prolonged systemic administration. Recently, two independent studies indicated that the cardioprotection associated with EPO treatment might be dose-dependent, with higher doses of Darbepoetin-α, an EPO analogue, producing better protection than lower doses against anterior wall thinning, LV dilatation and LV systolic dysfunction [29, 30]. However, prolonged EPO exposure

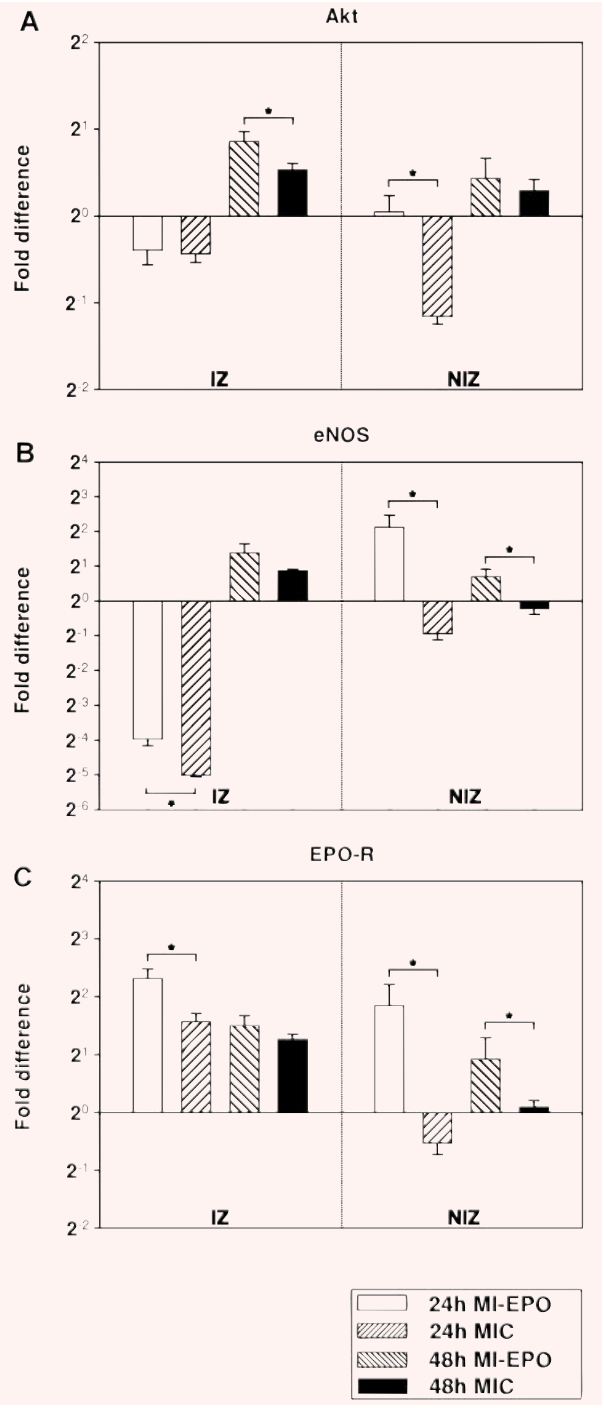

Fig. 6 EPO up-regulates mRNA of Akt, eNOS and EPO-R. (**A–C**) Quantitative real-time PCR analysis of Akt (**A**), eNOS (**B**) and EPO-R (**C**) in IZ and NIZ of MI-EPO ($n = 7$), MIC ($n = 7$) and Sham ($n = 7$) hearts. The average mRNA expression level of Akt, eNOS and EPO-R in the Sham hearts was arbitrarily given a value of 1 (2^0). $^*P < 0.05$.

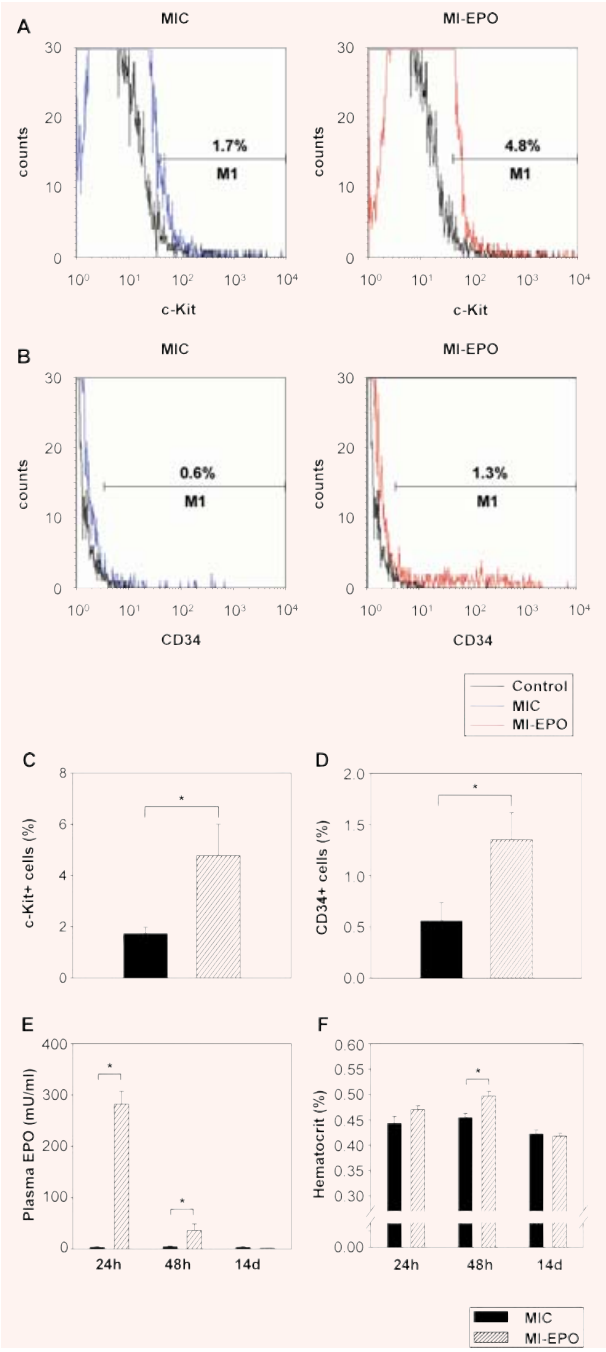

Fig. 7 Effects of local EPO delivery on peripheral blood. (**A–B**) Direct administration of EPO mobilizes c-Kit$^+$ and CD34$^+$ cells to the peripheral blood at 24 hrs. Representative FACS plots of c-Kit$^+$ (upper panel) and CD34$^+$ (lower panel) populations within peripheral blood in MIC and MI-EPO. (**C, D**) Percentage of c-Kit$^+$ (left) and CD34$^+$ (right) cells within the nucleated cell fraction of peripheral blood in MIC ($n = 7$) and MI-EPO ($n = 7$). (**E, F**) Kinetics of plasma EPO level (**E**) and haematocrit (**F**) at 24 hrs, 48 hrs and 2 weeks (MIC $n = 7,7,5$; MI-EPO $n = 7,7,5$). $^*P < 0.05$.

is likely to cause significant adverse effects on haematocrit and blood flow properties, resulting in vascular thrombosis and even excess mortality [31, 32]. In this study, EPO treatment was accomplished with a single intracardiac injection, which did not lead to intramural thrombus formation or abnormal effects on haematocrit. Moreover, circulating EPO levels were traced and side effects on haematocrit and thrombus formation in other organs have not been observed (data not shown). We suggest that a single, intracardiac administration of EPO may represent an alternative to systemic delivery, reducing the dose required for effective cardioprotection and minimizing side effects by limiting the potential for systemic toxicity and vascular thrombosis.

The underlying mechanism by which intracardiac injection of EPO improves cardiac function after MI has not been clearly identified, but there are several possible factors: (1) Reduction of infarction size and increase in capillary density may have preserved the myocardium. (2) Mobilization of CD34$^+$ and c-Kit$^+$ stem/progenitor cells in peripheral blood was enhanced at 24 hrs. (3) SDF-1α up-regulation at 24 hrs induced the early recruitment of stem/progenitor cells to the infarcted heart, which may, at least in part, have contributed to cardiac regeneration. (4) Additionally, EPO-mediated anti-inflammatory and protective effects may have limited myocardial damage and scar tissue formation.

The EPO-mediated directional migration of stem cells to the infarcted myocardium was particularly important. The SDF-1 and CXCR-4 ligand/receptor pair plays a pivotal role in stem cell migration [33, 34]. Early CXCR4$^+$ tissue-committed stem/progenitor cells (TCSCs) reside in the normal BM. CXCR4$^+$ haematopoietic stem cells (HSCs; also positive for CD34 or c-Kit) and TCSCs of BM could follow the SDF-1 gradient, become mobilized into peripheral blood and subsequently take part in angiogenesis and cardiac functional restoration [35–37]. It has been proposed that there is an extensive overlap in the expressions of haematopoietic and endothelial markers, suggesting a close developmental relationship between HSCs and EPCs [11, 12, 15, 38]. Reports also suggest that stem cells could incorporate into sites of active neovascularization after myocardial ischaemia [13, 14, 16, 17], and that EPO treatment significantly mobilized CD34$^+$/CD45$^+$ BM progenitor cells into the peripheral blood [18, 20]. Prunier *et al.* demonstrated that delayed EPO therapy could reduce post-MI cardiac remodelling only at a dose that mobilizes EPCs [30]. However, it remains unclear whether stem/progenitor cells mobilized by EPO could migrate to the ischaemic area to promote neovascularization and cardiac regeneration. The current study provides the first evidence demonstrating an early, temporally spatially distributed up-regulation of SDF-1 in EPO-treated hearts. The mobilization of c-Kit$^+$ and CD34$^+$ stem/progenitor cells into the peripheral blood and the significant recruitment of c-Kit$^+$ and CD34$^+$ stem cells in the infarcted heart might be associated with the SDF-1 up-regulation. EPO-R, CXCR-4 and eNOS were up-regulated, whereas MMP-2, which is essential for microenvironmental adhesion, maturation and differentiation of stem cells [39], was also increased. Hence, we postulate that intracardiac EPO injection may drive targeted stem cell mobilization to the injured heart, where the recruited stem cells might support functional tissue

formation. Recent studies suggested that c-Kit$^+$ and CD34$^+$ stem cells play a critical role in myocardial regeneration after infarction [40, 41]. However, it is not clear whether the enhanced stem cell recruitment contributes directly to the restored cardiac function and if to what extent. Furthermore, although the present data indicated the ability of EPO to mobilize stem cells to the infarct area and to generate survival signal through Akt and eNOS, more studies are needed to investigate the relation between stem cells in the infarct area and the generation of survival signal.

Despite our encouraging findings, the exact effects of EPO on the endogenous cardiac stem cells (CSCs) are still not clear. EPO has been shown to regulate the proliferation and differentiation of embryonic and adult neural stem cells *in vitro* and *in vivo* [42]. In addition, it is known that adult CSCs, negative for the expression of blood lineage markers (Lin$^-$) but positive for stem cell marker c-Kit, are multipotent and support myocardial regeneration [43]. Hence, it can be speculated that EPO delivered by intracardiac injection may also mediate CSCs proliferation and differentiation to regenerate the infarcted myocardium. Further studies need to be conducted in order to assess this hypothesis.

The molecular mechanisms associated with EPO-mediated cardiac protection have not been satisfactorily elucidated. We observed increases in the mRNA levels of pro-survival signal Akt and its downstream target eNOS at 24 and 48 hrs in MI-EPO rats, which might be closely associated with cardioprotective effects of EPO. This finding is in agreement with previous reports that EPO protects cardiomyocytes from apoptosis *via* up-regulation of eNOS and activation of Akt [44, 45]. The present data also confirm our previous finding that eNOS is crucial for SDF-1-mediated c-Kit$^+$ HSC directional migration [46]. One limitation of the current study is that, quantitative evaluation of Akt was restricted to the transcriptional level of the molecule. Akt activation indeed is mediated by phosphorylation without changes in the level of Akt protein [47]. Although Akt mRNA expression was transiently increased in EPO-treated hearts, it is difficult to estimate the level of activated phosphorylated Akt from mRNA level.

Interestingly, our finding that EPO-R mRNA was rapidly increased in EPO-treated cardiac tissue is consistent with a previous report that used a systemic approach [48], which suggests that EPO-R expression is independent of the EPO administration methods.

Others studies indicate that myocardial necrosis progresses within 6 hrs after the onset of MI [49, 50] and prompt reperfusion within this narrow time window significantly decreases early mortality [51]. Administration of EPO during the therapeutic window significantly reduces infarction size and improves cardiac function [3–5, 10, 32, 52]. Hence, local injection of EPO during emergency coronary artery bypass graft surgery after acute MI could be an optimal approach for EPO treatment.

In conclusion, intracardiac EPO administration augmented early stem cell recruitment to the ischaemic myocardium. This study strongly suggests that the beneficial effects of EPO treatment might be closely associated with the targeted migration of stem/progenitor cells. Further development of the concept will reveal whether these encouraging animal data can be translated into clinical applications.

Clinical perspective

This study demonstrates that EPO therapy is effective and feasible when delivered directly into the myocardium using a clinically relevant approach. The results reported herein establish EPO as a stem cell modulating hormone that facilitates cardiac regeneration. The effective pharmacological agents (such as EPO) that may be applied during coronary interventions or cardiac surgery to promote early cardiac preservation and stem cell activation are highly desirable. In addition, rapid recanalization of the occluded coronary artery is presently the best clinical approach to the treatment of acute MI. Accordingly, our present findings have obvious translational implications for the treatment of patients with acute coronary syndrome.

Acknowledgements

We thank Ms. Margit Fritsche, Ms. Miriam Nickel, Ms. Ann Katrin Hellberg, Ms. Nicole Deinet, Ms. Nicole Braun and Mr. Stefan Hinz, Institute of Clinical Chemistry and Laboratory Medicine and Institute of Pathology, University of Rostock, for their excellent technical assistance. We are grateful to Prof. Brigitte Vollmar, Prof. Matthias Peuster, Dr. Andreas Drynda and Dr. Barbara Nebe for their helpful discussion. This study was part of the thesis of D. Furlani submitted in fulfilment of the requirements for the degree of Doctor of Philosophy at the University of Rostock (Germany).

Sources of Funding

This work was supported by the German Helmholtz Association, Mecklenburg-Vorpommern (Nachwuchsgruppe Regenerative Medizin Regulation der Stammzellmigration 0402710), German Federal Ministry of Education and Research, BioChancePlus program (0313191), German Research Foundation, Sonderforschungsbereich/Transregio 7, B5, B2 and A4 and START-MSC (project 6: Kardiovaskuläre Differenzierung und Applikation definierter mesenchymaler Stammzellpopulationen), DAAD Project Based Personnel Exchange Programme with China.

Disclosures

None.

Supporting Information

Additional Supporting Information may be found in the online version of this article.

Table S1. Applied Biosystems TaqMan Gene Expression Assays used in quantitative real-time PCR

References

1. **Jelkmann W, Wagner K.** Beneficial and ominous aspects of the pleiotropic action of erythropoietin. *Ann Hematol.* 2004; 83: 673–86.
2. **Zwezdaryk KJ, Coffelt SB, Figueroa YG, Liu J, Phinney DG, LaMarca HL, Florez L, Morris CB, Hoyle GW, Scandurro AB.** Erythropoietin, a hypoxia-regulated factor, elicits a pro-angiogenic program in human mesenchymal stem cells. *Exp Hematol.* 2007; 35: 640–52.
3. **Calvillo L, Latini R, Kajstura J, Leri A, Anversa P, Ghezzi P, Salio M, Cerami A, Brines M.** Recombinant human erythropoietin protects the myocardium from ischemia-reperfusion injury and promotes beneficial remodeling. *Proc Natl Acad Sci USA.* 2003; 100: 4802–6.
4. **Parsa CJ, Matsumoto A, Kim J, Riel RU, Pascal LS, Walton GB, Thompson RB, Petrofski JA, Annex BH, Stamler JS, Koch WJ.** A novel protective effect of erythropoietin in the infarcted heart. *J Clin Invest.* 2003; 112: 999–1007.
5. **Tramontano AF, Muniyappa R, Black AD, Blendea MC, Cohen I, Deng L, Sowers JR, Cutaia MV, El-Sherif N.** Erythropoietin protects cardiac myocytes from hypoxia-induced apoptosis through an Akt-dependent pathway. *Biochem Biophys Res Commun.* 2003; 308: 990–4.
6. **Vandervelde S, van Luyn MJ, Tio RA, Harmsen MC.** Signaling factors in stem cell-mediated repair of infarcted myocardium. *J Mol Cell Cardiol.* 2005; 39: 363–76.
7. **Moon C, Krawczyk M, Ahn D, Ahmet I, Paik D, Lakatta EG, Talan MI.** Erythropoietin reduces myocardial infarction and left ventricular functional decline after coronary artery ligation in rats. *Proc Natl Acad Sci USA.* 2003; 100: 11612–7.
8. **Asaumi Y, Kagaya Y, Takeda M, Yamaguchi N, Tada H, Ito K, Ohta J, Shiroto T, Shirato K, Minegishi N, Shimokawa H.** Protective role of endogenous erythropoietin system in nonhematopoietic cells against pressure overload-induced left ventricular dysfunction in mice. *Circulation.* 2007; 115: 2022–32.
9. **Cai Z, Manalo DJ, Wei G, Rodriguez ER, Fox-Talbot K, Lu H, Zweier JL, Semenza GL.** Hearts from rodents exposed to intermittent hypoxia or erythropoietin are protected against ischemia-reperfusion injury. *Circulation.* 2003; 108: 79–85.
10. **Lipsic E, van der Meer P, Henning RH, Suurmeijer AJ, Boddeus KM, van Veldhuisen DJ, van Gilst WH, Schoemaker RG.** Timing of erythropoietin treatment for cardioprotection in ischemia/reperfusion. *J Cardiovasc Pharmacol.* 2004; 44: 473–9.
11. **Asahara T, Masuda H, Takahashi T, Kalka C, Pastore C, Silver M, Kearne M, Magner M, Isner JM.** Bone marrow origin of endothelial progenitor cells responsible for postnatal vasculogenesis in physiological and pathological neovascularization. *Circ Res.* 1999; 85: 221–8.
12. **Crosby JR, Kaminski WE, Schatteman G, Martin PJ, Raines EW, Seifert RA, Bowen-Pope DF.** Endothelial cells of hematopoietic origin make a significant contribution to adult blood vessel formation. *Circ Res.* 2000; 87: 728–30.
13. **Kalka C, Masuda H, Takahashi T, Kalka-Moll WM, Silver M, Kearney M, Li T, Isner JM, Asahara T.** Transplantation of *ex vivo* expanded endothelial progenitor cells for therapeutic neovascularization. *Proc Natl Acad Sci USA.* 2000; 97: 3422–7.
14. **Takahashi T, Kalka C, Masuda H, Chen D, Silver M, Kearney M, Magner M, Isner JM, Asahara T.** Ischemia- and cytokine-induced mobilization of bone marrow-derived endothelial progenitor cells for neovascularization. *Nat Med.* 1999; 5: 434–8.
15. **Schatteman GC, Hanlon HD, Jiao C, Dodds SG, Christy BA.** Blood-derived angioblasts accelerate blood-flow restoration in diabetic mice. *J Clin Invest.* 2000; 106: 571–8.
16. **Edelberg JM, Tang L, Hattori K, Lyden D, Rafii S.** Young adult bone marrow-derived endothelial precursor cells restore aging-impaired cardiac angiogenic function. *Circ Res.* 2002; 90: E89–93.
17. **Kawamoto A, Gwon HC, Iwaguro H, Yamaguchi JI, Uchida S, Masuda H, Silver M, Ma H, Kearney M, Isner JM, Asahara T.** Therapeutic potential of *ex vivo* expanded endothelial progenitor cells for myocardial ischemia. *Circulation.* 2001; 103: 634–7.
18. **Heeschen C, Aicher A, Lehmann R, Fichtlscherer S, Vasa M, Urbich C, Mildner-Rihm C, Martin H, Zeiher AM, Dimmeler S.** Erythropoietin is a potent physiologic stimulus for endothelial progenitor cell mobilization. *Blood.* 2003; 102: 1340–6.
19. **Bahlmann FH, DeGroot, K., Duckert T, Niemczyk E, Bahlmann E, Boehm SM, Haller H, Fliser D.** Endothelial progenitor cell proliferation and differentiation is regulated by erythropoietin. *Kidney Int.* 2003; 64: 1648–52.
20. **Bahlmann FH, De Groot K, Spandau JM, Landry AL, Hertel B, Duckert T, Boehm SM, Menne J, Haller H, Fliser D.** Erythropoietin regulates endothelial progenitor cells. *Blood.* 2004; 103: 921–6.
21. **George J, Goldstein E, Abashidze A, Wexler D, Hamed S, Shmilovich H, Deutsch V, Miller H, Keren G, Roth A.** Erythropoietin promotes endothelial progenitor cell proliferative and adhesive properties in a PI 3-kinase-dependent manner. *Cardiovasc Res.* 2005; 68: 299–306.
22. **Livak KJ, Schmittgen TD.** Analysis of relative gene expression data using real-time quantitative PCR and the 2(-Delta Delta C(T)) Method. *Methods.* 2001; 25: 402–8.
23. **Hessel M H, Steendijk, P, den Adel, B, Schutte C I, van der Laarse A.** Characterization of right ventricular function after monocrotaline-induced pulmonary hypertension in the intact rat. *Am J Physiol Heart Circ Physiol.* 2006; 291: H2424–30.
24. **Agata, J, Chao, L, Chao J.** Kallikrein gene delivery improves cardiac reserve and attenuates remodeling after myocardial infarction. *Hypertension.* 2002; 40: 653–9.
25. **Lindahl B, Toss H, Siegbahn A, Venge P, Wallentin L.** Markers of myocardial damage and inflammation in relation to long-term mortality in unstable coronary artery disease. FRISC Study Group. Fragmin during

Instability in Coronary Artery Disease. *N Engl J Med.* 2000; 343: 1139–47.

26. **Moller JE, Hillis GS, Oh JK, Pellikka PA.** Prognostic importance of secondary pulmonary hypertension after acute myocardial infarction. *Am J Cardiol.* 2005; 96: 199–203.
27. **Nishiya, D, Omura, T, Shimada, K, Matsumoto, R, Kusuyama, T, Enomoto, S, Iwao, H, Takeuchi, K, Yoshikawa, J, Yoshiyama M.** Effects of erythropoietin on cardiac remodeling after myocardial infarction. *J Pharmacol Sci.* 2006; 101: 31–9.
28. **Jasmin JF, Calderone A, Leung TK, Villeneuve L, Dupuis J.** Lung structural remodeling and pulmonary hypertension after myocardial infarction: complete reversal with irbesartan. *Cardiovasc Res.* 2003; 58: 621–31.
29. **Gao E, Boucher M, Chuprun JK, Zhou RH, Eckhart AD, Koch WJ.** Darbepoetin alfa, a long-acting erythropoietin analog, offers novel and delayed cardioprotection for the ischemic heart. *Am J Physiol Heart Circ Physiol.* 2007; 293: H60–8.
30. **Prunier F, Pfister O, Hadri L, Liang L, Del Monte F, Liao R, Hajjar RJ.** Delayed erythropoietin therapy reduces post-MI cardiac remodeling only at a dose that mobilizes endothelial progenitor cells. *Am J Physiol Heart Circ Physiol.* 2007; 292: H522–9.
31. **Besarab A, Bolton WK, Browne JK, Egrie JC, Nissenson AR, Okamoto DM, Schwab SJ, Goodkin DA.** The effects of normal as compared with low hematocrit values in patients with cardiac disease who are receiving hemodialysis and epoetin. *N Engl J Med.* 1998; 339: 584–90.
32. **van der Meer P, Voors AA, Lipsic E, Smilde TD, van Gilst WH, van Veldhuisen DJ.** Prognostic value of plasma erythropoietin on mortality in patients with chronic heart failure. *J Am Coll Cardiol.* 2004; 44: 63–7.
33. **Ma N, Stamm C, Kaminski A, Li W, Kleine HD, Muller-Hilke B, Zhang L, Ladilov Y, Egger D, Steinhoff G.** Human cord blood cells induce angiogenesis following myocardial infarction in NOD/scidmice. *Cardiovasc Res.* 2005; 66: 45–54.
34. **Elmadbouh I, Haider H, Jiang S, Idris NM, Lu G, Ashraf M.** *Ex vivo* delivered stromal cell-derived factor-1alpha promotes stem cell homing and induces angiomyogenesis in the infarcted myocardium. *J Mol Cell Cardiol.* 2007; 42: 792–803.
35. **Losordo DW, Schatz RA, White CJ, Udelson JE, Veereshwarayya V, Durgin M, Poh KK, Weinstein R, Kearney M, Chaudhry M, Burg A, Eaton L, Heyd L, Thorne T, Shturman L, Hoffmeister P, Story K, Zak V, Dowling D, Traverse JH, Olson RE, Flanagan J, Sodano D, Murayama T, Kawamoto A, Kusano KF, Wollins J, Welt F, Shah P, Soukas P, Asahara T, Henry TD.** Intramyocardial transplantation of autologous CD34+ stem cells for intractable angina: a phase I/IIa double-blind, randomized controlled trial. *Circulation.* 2007; 115: 3165–72.
36. **Stamm C, Westphal B, Kleine HD, Petzsch M, Kittner C, Klinge H, Schumichen C, Nienaber CA, Freund M, Steinhoff G.** Autologous bone-marrow stem-cell transplantation for myocardial regeneration. *Lancet.* 2003; 361: 45–6.
37. **Ratajczak MZ, Kucia M, Reca R, Majka M, Janowska-Wieczorek A, Ratajczak J.** Stem cell plasticity revisited: CXCR4-positive cells expressing mRNA for early muscle, liver and neural cells 'hide out' in the bone marrow. *Leukemia.* 2004; 18: 29–40.
38. **Jaffredo T, Nottingham W, Liddiard K, Bollerot K, Pouget C, de Bruijn M.** From hemangioblast to hematopoietic stem cell: an endothelial connection? *Exp Hematol.* 2005; 33: 1029–40.
39. **Lapidot T, Dar A, Kollet O.** How do stem cells find their way home? *Blood.* 2005; 106: 1901–10.
40. **Cimini M, Fazel S, Zhuo S, Xaymardan M, Fujii H, Weisel RD, Li RK.** c-kit dysfunction impairs myocardial healing after infarction. *Circulation.* 2007; 116: I77–82.
41. **Kawamoto A, Iwasaki H, Kusano K, Murayama T, Oyamada A, Silver M, Hulbert C, Gavin M, Hanley A, Ma H, Kearney M, Zak V, Asahara T, Losordo DW.** CD34-positive cells exhibit increased potency and safety for therapeutic neovascularization after myocardial infarction compared with total mononuclear cells. *Circulation.* 2006; 114: 2163–9.
42. **Shingo T, Sorokan ST, Shimazaki T, Weiss S.** Erythropoietin regulates the *in vitro* and *in vivo* production of neuronal progenitors by mammalian forebrain neural stem cells. *J Neurosci.* 2001; 21: 9733–43.
43. **Beltrami AP, Barlucchi L, Torella D, Baker M, Limana F, Chimenti S, Kasahara H, Rota M, Musso E, Urbanek K, Leri A, Kajstura J, Nadal-Ginard B, Anversa P.** Adult cardiac stem cells are multipotent and support myocardial regeneration. *Cell.* 2003; 114: 763–76.
44. **Burger D, Lei M, Geoghegan-Morphet N, Lu X, Xenocostas A, Feng Q.** Erythropoietin protects cardiomyocytes from apoptosis *via* up-regulation of endothelial nitric oxide synthase. *Cardiovasc Res.* 2006; 72: 51–9.
45. **Feng Q.** Beyond erythropoiesis: the anti-inflammatory effects of erythropoietin. *Cardiovasc Res.* 2006; 71: 615–7.
46. **Kaminski A, Ma N, Donndorf P, Lindenblatt N, Feldmeier G, Ong LL, Furlani D, Skrabal CA, Liebold A, Vollmar B, Steinhoff G.** Endothelial NOS is required for SDF-1alpha/CXCR4-mediated peripheral endothelial adhesion of c-kit+ bone marrow stem cells. *Lab Invest.* 2008; 88: 58–69.
47. **Kobayashi, H, Minatoguchi, S, Yasuda, S, Bao, N, Kawamura, I, Iwasa, M, Yamaki, T, Sumi, S, Misao, Y, Ushikoshi, H, Nishigaki, K, Takemura, G, Fujiwara, T, Tabata, Y, Fujiwara H.** Post-infarct treatment with an erythropoietin-gelatin hydrogel drug delivery system for cardiac repair. *Cardiovasc Res.* 2008; 79: 611–20.
48. **Li Y, Takemura G, Okada H, Miyata S, Maruyama R, Li L, Higuchi M, Minatoguchi S, Fujiwara T, Fujiwara H.** Reduction of inflammatory cytokine expression and oxidative damage by erythropoietin in chronic heart failure. *Cardiovasc Res.* 2006; 71: 684–94.
49. **Reimer KA, Lowe JE, Rasmussen MM, Jennings RB.** The wavefront phenomenon of ischemic cell death. 1. Myocardial infarct size *versus* duration of coronary occlusion in dogs. *Circulation.* 1977; 56: 786–94.
50. **Hirayama A, Adachi T, Asada S, Mishima M, Nanto S, Kusuoka H, Yamamoto K, Matsumura Y, Hori M, Inoue M.** Late reperfusion for acute myocardial infarction limits the dilatation of left ventricle without the reduction of infarct size. *Circulation.* 1993; 88: 2565–74.
51. **Kocher AA, Schuster MD, Szabolcs MJ, Takuma S, Burkhoff D, Wang J, Homma S, Edwards NM, Itescu S.** Neovascularization of ischemic myocardium by human bone-marrow-derived angioblasts prevents cardiomyocyte apoptosis, reduces remodeling and improves cardiac function. *Nat Med.* 2001; 7: 430–6.
52. **Hirata A, Minamino T, Asanuma H, Fujita M, Wakeno M, Myoishi M, Tsukamoto O, Okada K, Koyama H, Komamura K, Takashima S, Shinozaki Y, Mori H, Shiraga M, Kitakaze M, Hori M.** Erythropoietin enhances neovascularization of ischemic myocardium and improves left ventricular dysfunction after myocardial infarction in dogs. *J Am Coll Cardiol.* 2006; 48: 176–84.